Electronic Supplementary Material (ESI) for Soft Matter.
This journal is © The Royal Society of Chemistry 2024

Supporting Information

Mechanical guidance of stem cells self-organization and pattern formation

Wei-Hua Zhou[a#], Lin-Ru Qiao[a#], She-Juan Xie[a], Zhuo Chang [a,*], Xu Yin [a*], and Guang-Kui Xu[a]

a. Laboratory for Multiscale Mechanics and Medical Science, Department of Engineering Mechanics, State Key Laboratory for Strength and Vibration of Mechanical Structures, Xi'an Jiaotong University, Xi'an 710049, China

[#]These authors contributed equally to this work.

* Corresponding authors: zhuochang@xjtu.edu.cn; 4120106049@stu.xjtu.edu.cn

S1. Derivation of mechanical model

The pattern is described by the concentration distribution of SCs, which varies with time and space and is represented by $n(x,t)$. The evolution of SCs is determined by three general equations:

$$\partial_t n = \nabla \cdot (n \partial_t u) + D\nabla^2 (n), \tag{S1}$$

$$\partial_t \rho = \nabla \cdot (\rho \partial_t u), \tag{S2}$$

$$s\frac{\partial_t u}{\rho} = \nabla\left[(\mu_1 \partial_t \varepsilon + \mu_2 \partial_t \theta I) + \frac{E}{1+\nu}\left(\varepsilon + \frac{\nu}{1-2\nu}\theta I\right)\right] + \nabla\left[\frac{\tau n}{1+\lambda n^2} I\right]. \tag{S3}$$

In addition, our simulation adopts periodic boundary conditions, specifically:

$$\vec{\theta} \cdot \nabla (n) = 0, \quad \nabla \rho (0,t) = 0, \quad u = 0 \tag{S4}$$

where $\vec{\theta}$ is the outer normal at the boundary. These configurations are established to guarantee the absence of flux and local displacement of cells at the boundary. More information on the expanded form and derivation process of the above equations are described as follows.

Equation S1 describes the change rate of SCs concentration, and can be expanded into the two-dimensional domain:

$$\partial_t n = \partial_x (n \partial_t U) + \partial_y (n \partial_t V) + D\nabla^2 (n), \tag{S5}$$

where U and V represent the components of displacement u in the x and y directions respectively. Similarly, Equation S2 represent the change rate of ECM and can be written as:

$$\partial_t \rho = \partial_x (\rho \partial_t U) + \partial_y (\rho \partial_t V), \tag{S6}$$

Equation S3 shows the dynamic mechanical balance between SCs-ECM-cultural environment, and the balance system is composed of internal and external forces:

$F_{\text{int}} + F_{\text{ext}} = 0$. The internal force F_{int} is described via the divergence of a stress tensor σ, as shown on the left side of Equation S3, where encompasses the active tractions of cells and the viscoelastic forces of the ECM. The external force F_{ext} is modeled as the viscous resistance force anchored on the substrate (culture dish). The expanded form of Equation S3 in the *x* and *y* directions can be represented as follows:

$$\begin{aligned}&\partial_x^2\left(\mu\partial_t U\right)+\left(\nu+1\right)\partial_x^2 U+\frac{\mu_1}{2}\partial_y^2\left(\partial_t U\right)+\frac{1}{2}\partial_y^2 U-\frac{s}{\rho}\partial_t U=\\&-\partial_x\left(\frac{\tau n}{1+\lambda n^2}\right)+\left(\frac{\mu_1}{2}-\mu\right)\partial_x\partial_y\left(\partial_t V\right)-\left(\nu+\frac{1}{2}\right)\partial_x\partial_y\left(V\right),\end{aligned} \tag{S7}$$

$$\begin{aligned}&\partial_y^2\left(\mu\partial_t V\right)+\left(\nu+1\right)\partial_y^2 V+\frac{\mu_1}{2}\partial_x^2\left(\partial_t V\right)+\frac{1}{2}\partial_x^2 V-\frac{s}{\rho}\partial_t V=\\&-\partial_y\left(\frac{\tau n}{1+\lambda n^2}\right)+\left(\frac{\mu_1}{2}-\mu\right)\partial_x\partial_y\left(\partial_t U\right)-\left(\nu+\frac{1}{2}\right)\partial_x\partial_y\left(U\right).\end{aligned} \tag{S8}$$

S2. Numerical implementations of the model

The domain is discretized into a 300 × 300 matrix, and the time is discretized, where $\mathrm{d}x = \mathrm{d}y = 0.25$ and $\mathrm{d}t = 0.006$.

Using (i, j) to describe points in the computational domain and discretize the Equation S6 by the upwind difference method, where $J^U = \rho\partial_t U$ and $J^V = \rho\partial_t V$:

$$\rho_{i,j}^{N+1} = \rho_{i,j}^{*} - \Delta t\frac{J^V_{i+1/2,j} - J^V_{i-1/2,j}}{\mathrm{d}x}, \tag{S9}$$

$$\rho_{i,j}^{*} = \rho_{i,j}^{N} - \Delta t\frac{J^U_{i,j+1/2} - J^U_{i,j-1/2}}{\mathrm{d}x}. \tag{S10}$$

where $J^U_{i,j+1/2}$ represents the value of the *x* component of the ECM flux between the points (i, j) and $(i, j+1)$, $J^V_{i+1/2,j}$ is defined by:

$$\begin{aligned}J^U_{i,j+1/2} &= \varpi^{N+1/2}_{i,j+1/2}\rho^N_{i,j+1} \quad \text{if} \quad \varpi^{N+1/2}_{i,j+1/2} > 0\\&= \varpi^{N+1/2}_{i,j+1/2}\rho^N_{i,j} \qquad\qquad\quad \varpi^{N+1/2}_{i,j+1/2} < 0\end{aligned}, \tag{S11}$$

$$\varpi_{i,j+1/2}^{N+1/2}=\frac{1}{2}\left(\frac{U_{i,j}^{N+1}-U_{i,j}^{N}}{\mathrm{d}t}+\frac{U_{i,j+1}^{N+1}-U_{i,j+1}^{N}}{\mathrm{d}t}\right). \tag{S12}$$

$$\begin{aligned} J_{i+1/2,j}^{V} &= \upsilon_{i+1/2,j}^{N+1/2}\rho_{i+1,j}^{*} \quad \text{if} \quad \upsilon_{i+1/2,j}^{N+1/2}>0 \\ &= \upsilon_{i+1/2,j}^{N+1/2}\rho_{i,j}^{*} \quad\quad\quad\quad \upsilon_{i+1/2,j}^{N+1/2}<0 \end{aligned}, \tag{S13}$$

$$\upsilon_{i+1/2,j}^{N+1/2}=\frac{1}{2}\left(\frac{V_{i,j}^{N+1}-V_{i,j}^{N}}{\mathrm{d}t}+\frac{V_{i+1,j}^{N+1}-V_{i+1,j}^{N}}{\mathrm{d}t}\right). \tag{S14}$$

Different from the calculation of local ECM concentration change rate, the local SCs concentration change rate (Equation S1) affects the diffusion term by:

$$\begin{aligned} &D\nabla^2(n)=\partial_x^2(n)+\partial_y^2(n) \\ &=\frac{[n(i+1,j)+n(i-1,j)+n(i,j+1)+n(i,j-1)]-4n(i,j)}{dxdy}\cdot \end{aligned} \tag{S15}$$

Discretizing Equation S1 by the upwind difference method:

$$n_{i,j}^{N+1}=n_{i,j}^{**}+D\nabla^2(n). \tag{S16}$$

$$n_{i,j}^{*}=n_{i,j}^{N}-\Delta t\frac{J_{i,j+1/2}^{U}-J_{i,j-1/2}^{U}}{\mathrm{d}x}, \tag{S17}$$

$$\begin{aligned} J_{i,j+1/2}^{U} &= \upsilon_{i,j+1/2}^{N+1/2}n_{i,j+1}^{N} \quad \text{if} \quad \upsilon_{i,j+1/2}^{N+1/2}>0 \\ &= \upsilon_{i,j+1/2}^{N+1/2}\rho n_{i,j}^{N} \quad\quad\quad\quad \upsilon_{i,j+1/2}^{N+1/2}<0 \end{aligned}, \tag{S18}$$

$$n_{i,j}^{**}=n_{i,j}^{*}-\Delta t\frac{J_{i+1/2,j}^{V}-J_{i-1/2,j}^{V}}{\mathrm{d}x}, \tag{S19}$$

$$\begin{aligned} J_{i+1/2,j}^{V} &= \varpi_{i+1/2,j}^{N+1/2}n_{i+1,j}^{*} \quad \text{if} \quad \varpi_{i+1/2,j}^{N+1/2}>0 \\ &= \varpi_{i+1/2,j}^{N+1/2}n_{i,j}^{*} \quad\quad\quad\quad \varpi_{i+1/2,j}^{N+1/2}<0 \end{aligned}. \tag{S20}$$

Taking the x-direction as an example, the SCs-ECM-cultural environment mechanical equilibrium (Equation S7) is expanded as Crank-Nicolson scheme:

$$\begin{aligned} &A\partial_x^2(\partial_t U)+B\partial_y^2(\partial_t U)+C\partial_x^2 U+D\partial_y^2 U+E\partial_t U= \\ &F_x(\mathrm{n})+W\partial_x\partial_y V+Y\partial_x\partial_y(\partial_t V) \end{aligned}. \tag{S21}$$

where $A=\mu$; $B=\mu_1/2$; $C=\nu+1$; $D=0.5$; $E=-s/\rho$; $F(n)=n/(1+\lambda n^2)$;

$W=-\left(1/2+\nu\right);Y=(\mu_1/2-\mu)$. The equation (Equation S21) is discretized in the following form to facilitate computational analysis:

$$\partial_t U=\frac{U^{N+1}-U^N}{\Delta t}, \tag{S22}$$

$$\begin{aligned}\partial_t^2 U=\frac{\partial^2 U}{\partial t^2}=\frac{U_t^{N+1}-U_t^N}{\Delta t}=\frac{\frac{U^{N+2}-U^{N+1}}{\Delta t}-\frac{U^{N+1}-U^N}{\Delta t}}{\Delta t}\\ =\frac{U^{N+2}-2U^{N+1}+U^N}{\Delta t^2}=\frac{U^{N+1}-2U^N+U^{N-1}}{\Delta t^2}\end{aligned}, \tag{S23}$$

$$\partial_x^2 U_{i,j}=\frac{1}{\mathrm{d}x^2}\left(U_{i,j-1}-2U_{i,j}+U_{i,j+1}\right), \tag{S24}$$

$$\partial_y^2 U_{i,j}=\frac{1}{\mathrm{d}y^2}\left(U_{i-1,j}-2U_{i,j}+U_{i+1,j}\right), \tag{S25}$$

$$\partial_x\partial_y U_{i,j}=\frac{1}{4\mathrm{d}x\mathrm{d}y}\left(U_{i+1,j+1}+U_{i-1,j-1}-U_{i-1,j+1}+U_{i+1,j-1}\right). \tag{S26}$$

The discretized equation is:

$$\begin{aligned}&A\frac{\partial_x^2 U_{i,j}^{N+1}-\partial_x^2 U_{i,j}^N}{\mathrm{d}t}+B\frac{\partial_y^2 U_{i,j}^{N+1}-\partial_y^2 U_{i,j}^N}{\mathrm{d}t}+\\ &C\frac{\partial_x^2 U_{i,j}^{N+1}+\partial_x^2 U_{i,j}^N}{2}+D\frac{\partial_y^2 U_{i,j}^{N+1}+\partial_y^2 U_{i,j}^N}{2}+\\ &E\frac{1}{k}\left(U_{i,j}^{N+1}-U_{i,j}^N\right)=\frac{F_x(n^{N+1})+F_x(n^N)}{2}+\\ &\mathrm{W}\frac{\partial_x\partial_y V_{i,j}^{N+1}+\partial_x\partial_y V_{i,j}^N}{2}+\mathrm{Y}\frac{\partial_x\partial_y V_{i,j}^{N+1}-\partial_x\partial_y V_{i,j}^N}{\mathrm{d}t}\end{aligned}. \tag{S27}$$

Expansion of the above equation leads to:

$$
\begin{aligned}
&\frac{A}{k}\frac{1}{\mathrm{d}x^2}\left[\left(U_{i,j-1}^{N+1}-2U_{i,j}^{N+1}+U_{i,j+1}^{N+1}\right)-\left(U_{i,j-1}^{N}-2U_{i,j}^{N}+U_{i,j+1}^{N}\right)\right]+\\
&\frac{B}{k}\frac{1}{\mathrm{d}x^2}\left[\left(U_{i-1,j}^{N+1}-2U_{i,j}^{N+1}+U_{i+1,j}^{N+1}\right)-\left(U_{i-1,j}^{N}-2U_{i,j}^{N}+U_{i+1,j}^{N}\right)\right]+\\
&\frac{C}{2}\frac{1}{\mathrm{d}x^2}\left[\left(U_{i,j-1}^{N+1}-2U_{i,j}^{N+1}+U_{i,j+1}^{N+1}\right)+\left(U_{i-1,j}^{N}-2U_{i,j}^{N}+U_{i+1,j}^{N}\right)\right]+\\
&\frac{D}{2}\frac{1}{\mathrm{d}x^2}\left[\left(U_{i-1,j}^{N+1}-2U_{i,j}^{N+1}+U_{i+1,j}^{N+1}\right)+\left(U_{i-1,j}^{N}-2U_{i,j}^{N}+U_{i+1,j}^{N}\right)\right]+\\
&\frac{E}{\mathrm{d}t}\left(U_{i,j}^{N+1}-U_{i,j}^{N}\right)=\\
&\frac{1}{2}\frac{1}{2\mathrm{d}x}\left[\left(\frac{\tau n_{i,j-1}^{N+1}}{1+\alpha(n_{i,j-1}^{N+1})^2}-\frac{\tau n_{i,j+1}^{N+1}}{1+\alpha(n_{i,j+1}^{N+1})^2}\right)+\left(\frac{\tau n_{i,j-1}^{N}}{1+\alpha(n_{i,j-1}^{N})^2}-\frac{\tau n_{i,j+1}^{N}}{1+\alpha(n_{i,j+1}^{N})^2}\right)\right]+\\
&\frac{W}{2}\frac{1}{4\mathrm{d}x\mathrm{d}y}[\left(V_{i+1,j+1}^{N+1}+V_{i-1,j-1}^{N+1}-V_{i+1,j-1}^{N+1}-V_{i-1,j+1}^{N+1}\right)+\\
&\left(V_{i+1,j+1}^{N}+V_{i-1,j-1}^{N}-V_{i+1,j-1}^{N}-V_{i-1,j+1}^{N}\right)]+\\
&\frac{Y}{k}\frac{1}{4\mathrm{d}x\mathrm{d}y}[\left(V_{i+1,j+1}^{N+1}+V_{i-1,j-1}^{N+1}-V_{i+1,j-1}^{N+1}-V_{i-1,j+1}^{N+1}\right)-\\
&\left(V_{i+1,j+1}^{N}+V_{i-1,j-1}^{N}-V_{i+1,j-1}^{N}-V_{i-1,j+1}^{N}\right)] \qquad .
\end{aligned}
\tag{S28}
$$

The simplified form of the above equation is:

$$
(a_{ij}U_{i,j-1}^{N+1}+b_{ij}U_{i-1,j}^{N+1}+c_{ij}U_{i,j}^{N+1}+d_{ij}U_{i+1,j}^{N+1}+e_{ij}U_{i,j+1}^{N+1})=q_{ij}^{(1)}. \tag{S29}
$$

where:

$$
a_{ij}=\frac{1}{\mathrm{d}x^2}(\mu+\frac{\mathrm{d}t}{2}(1+\nu)), \tag{S30}
$$

$$
b_{ij}=\frac{1}{2\mathrm{d}x^2}(\mu_1+\frac{\mathrm{d}t}{2}), \tag{S31}
$$

$$
c_{ij}=-\frac{2}{\mathrm{d}x^2}\left[\mu+\frac{\mathrm{d}t}{2}(1+\nu)+\frac{1}{2}(\mu_1+\frac{\mathrm{d}t}{2})\right]-s\left(\rho_{ij}^{N+1}\right)^{-1}, \tag{S32}
$$

$$
d_{ij}=\frac{1}{2\mathrm{d}x^2}(\mu_1+\frac{\mathrm{d}t}{2}), \tag{S33}
$$

$$
e_{ij}=\frac{1}{\mathrm{d}x^2}(\mu+\frac{\mathrm{d}t}{2}(1+\nu)), \tag{S34}
$$

$$q_{ij}^{(1)}=\frac{k}{4\mathrm{d}x}\left(\frac{\tau n_{i,j-1}^{N}}{1+\alpha(n_{i,j-1}^{N})^{2}}-\frac{\tau n_{i,j+1}^{N}}{1+\alpha(n_{i,j+1}^{N})^{2}}+\frac{\tau n_{i,j-1}^{N+1}}{1+\alpha(n_{i,j-1}^{N+1})^{2}}-\frac{\tau n_{i,j+1}^{N+1}}{1+\alpha(n_{i,j+1}^{N+1})^{2}}\right)+$$
$$\frac{1}{4\mathrm{d}x^{2}}\left(\frac{\mu_{1}}{2}-\mu\right)[(V_{i+1,j+1}^{N+1}+V_{i-1,j-1}^{N+1}-V_{i+1,j-1}^{N+1}-V_{i-1,j+1}^{N+1})-$$
$$\left(V_{i+1,j+1}^{N}+V_{i-1,j-1}^{N}-V_{i+1,j-1}^{N}-V_{i-1,j+1}^{N}\right)] \quad . \tag{S35}$$
$$-\frac{\mathrm{d}t}{8\mathrm{d}x^{2}}(\frac{1}{2}+\nu)[(V_{i+1,j+1}^{N+1}+V_{i-1,j-1}^{N+1}-V_{i+1,j-1}^{N+1}-V_{i-1,j+1}^{N+1})+$$
$$\left(V_{i+1,j+1}^{N}+V_{i-1,j-1}^{N}-V_{i+1,j-1}^{N}-V_{i-1,j+1}^{N}\right)]$$

Similarly, the mechanical balance equation in y-direction is:

$$(b_{ij}V_{i,j-1}^{N+1}+a_{ij}V_{i-1,j}^{N+1}+c_{ij}V_{i,j}^{N+1}+e_{ij}V_{i+1,j}^{N+1}+d_{ij}V_{i,j+1}^{N+1})=q_{ij}^{(2)}. \tag{S36}$$

In this form, the local SCs-ECM-cultural environment equilibrium equation can be solved by the D03EBF algorithm of NAG toolbox in MATLAB to obtain the next step U^{N+1}, V^{N+1} through the method of circular approximation approximate solution.

S3. Direction distribution of experimentally generated patterns in

Section 3.1 and Figure 1

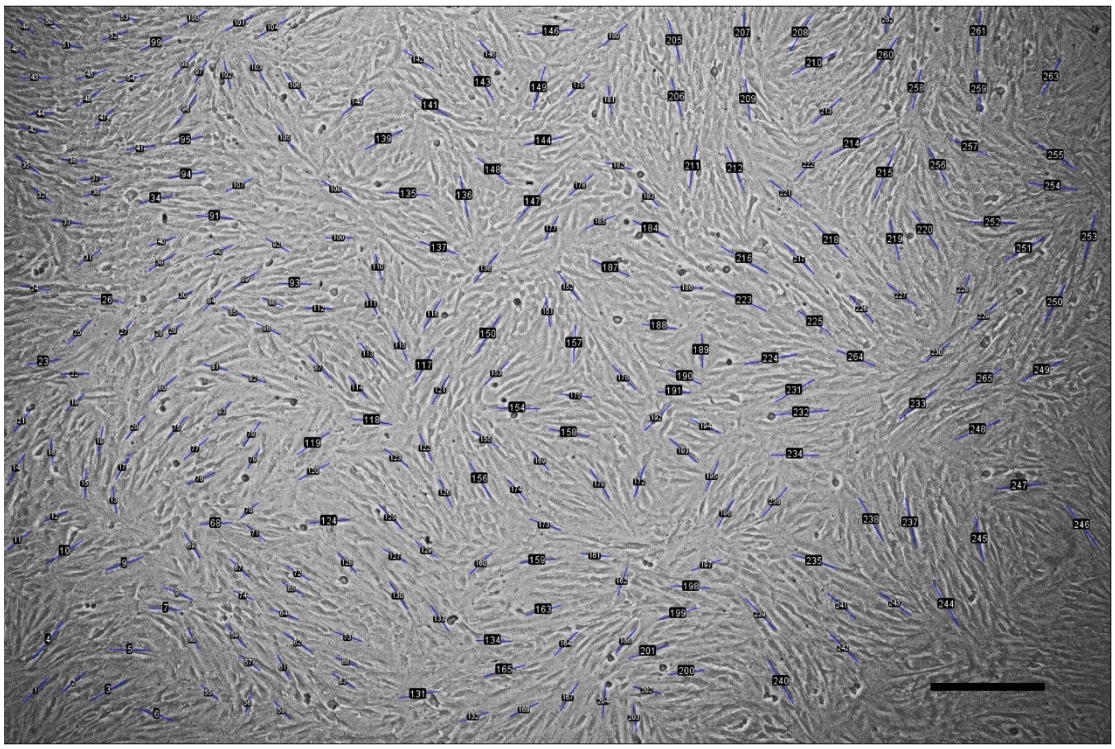

Fig. S1 Mark the direction of cell aggregates in generating patterns without geometric constraints, Scale bars are 200μm.

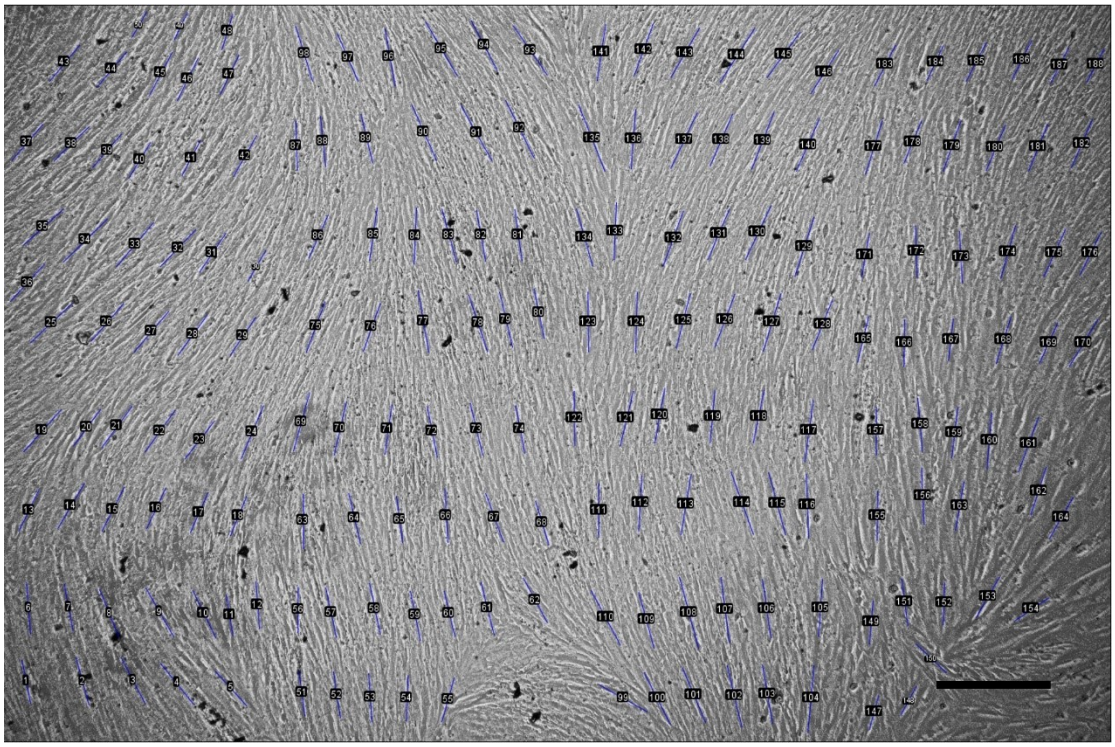

Fig. S2 Mark the direction of cell aggregates in generating patterns with geometric constraints $\alpha = 0^{\circ}$, Scale bars are 200μm.

S4. SCs Pattern under various geometric constraint directions

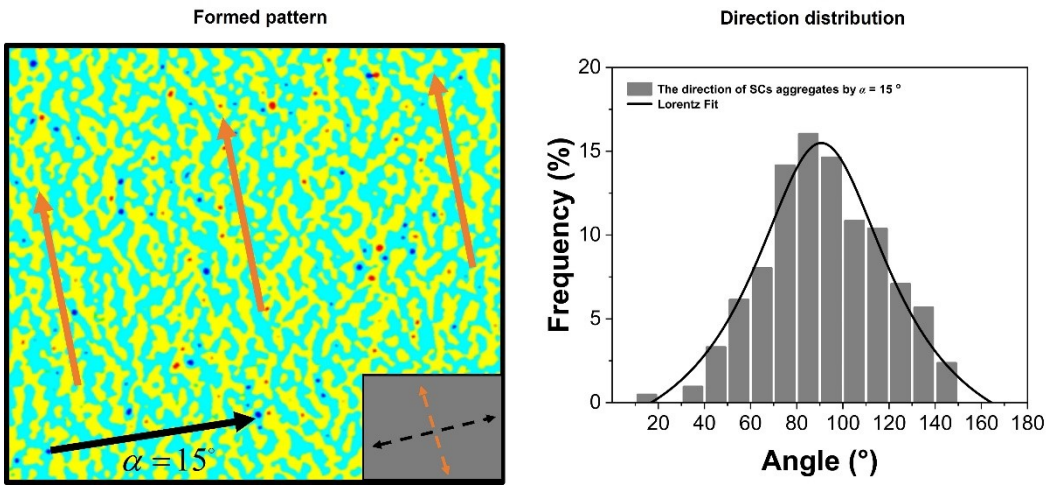

Fig. S3 SCs Pattern under geometric constraint directions $\alpha = 15^{\circ}$.

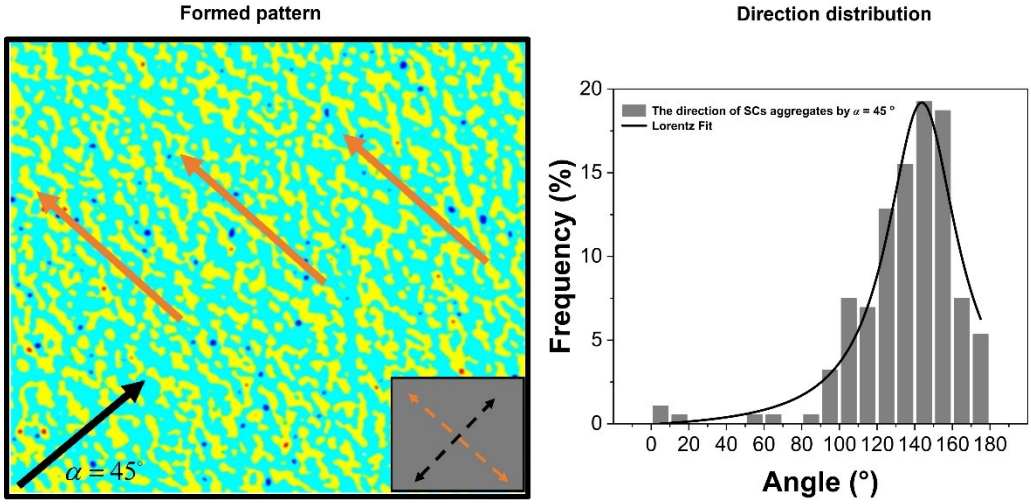

Fig. S4 SCs Pattern under geometric constraint directions $\alpha = 45^{\circ}$.

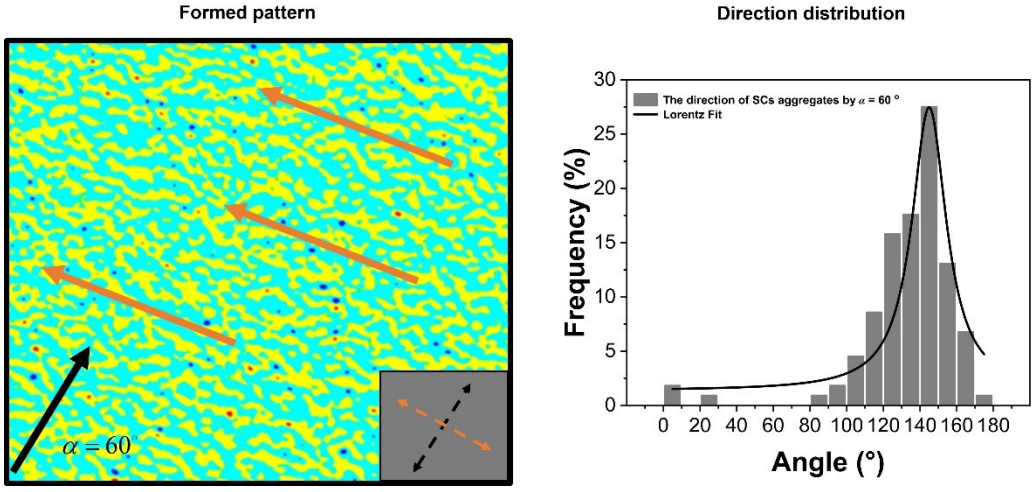

Fig. S5 SCs Pattern under geometric constraint directions $\alpha = 60^{\circ}$.

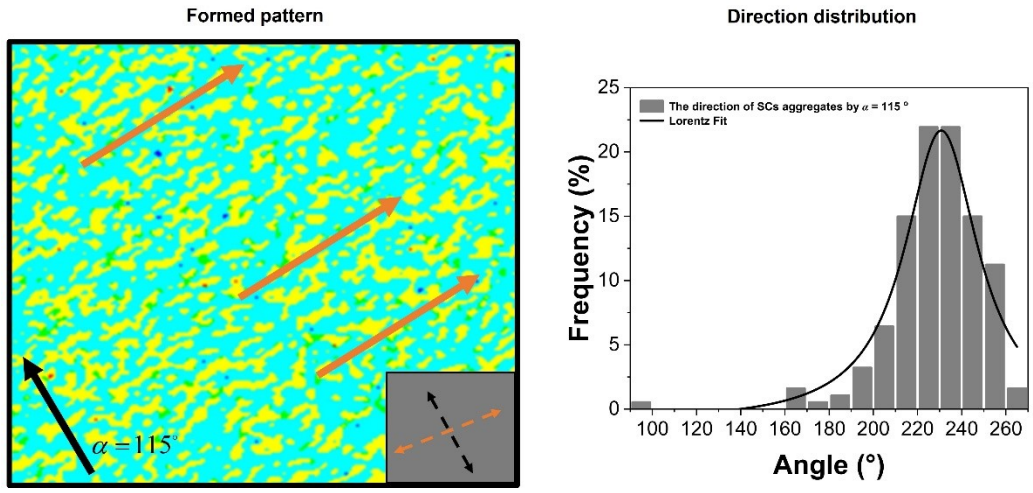

Fig. S6 SCs Pattern under geometric constraint directions $\alpha = 115^{o}$.

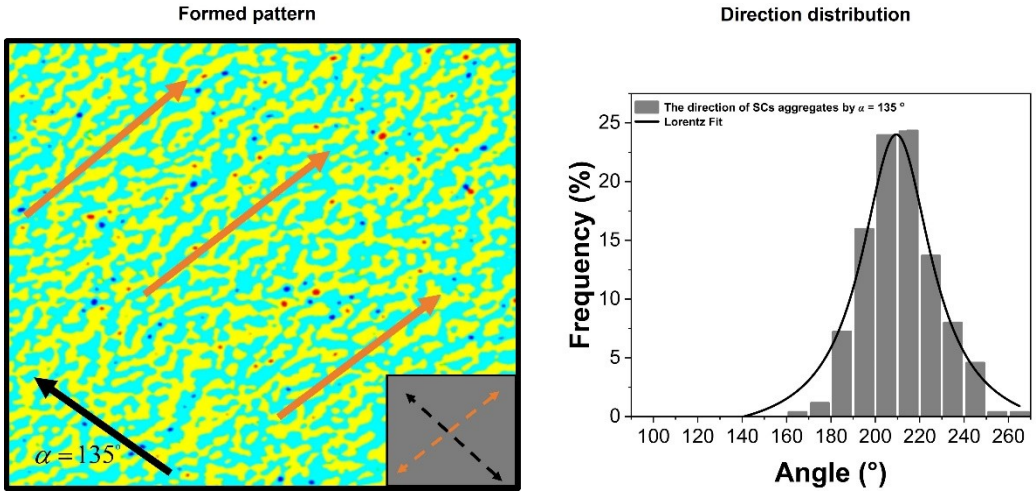

Fig. S7 SCs Pattern under geometric constraint directions $\alpha = 135^{o}$.

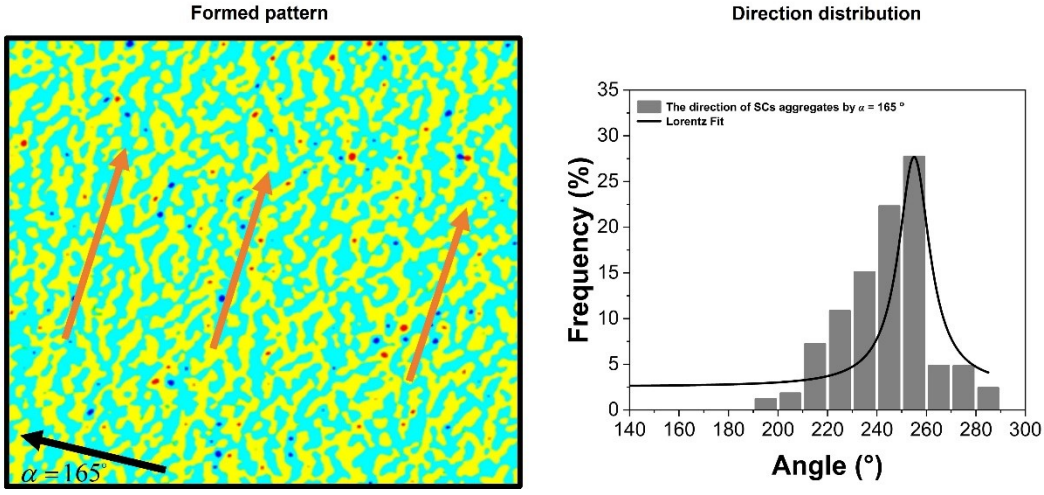

Fig. S8 SCs Pattern under geometric constraint directions $\alpha = 165^{o}$.